J Genet Resour2026; 12(1): 41-52 *Homepage: http://sc.journals.umz.ac.ir/*

RESEARCH ARTICLE *DOI: 10.22080/jgr.2026.31450.1459*

Co-upregulation of *MEG3* and *TUG1* lncRNAs by Hyaluronic Acid-based Nanoparticles Confers Selective Toxicity in Lung Adenocarcinoma

Fatemeh Mehraban[1], Nahid Babaei[1,*], Amir Jalali[2,*], Ali Salehzadeh[3] and Abdolhassan Doulah[4]

[1] Department of Molecular Cell Biology and Genetics, Bu.C., Islamic Azad University, Bushehr, Iran
[2] Department of Biology, Faculty of Sciences, Arak University, Arak, Iran
[3]Department of Biology, Ra.C., Islamic Azad University, Rasht, Iran
[4]Department of Biology, Bu.C., Islamic Azad University, Bushehr, Iran

ARTICLE INFO

Article history:
Received 23 November 2025
Accepted 25 December 2025
Available 17 January 2026

Keywords:
CD44 targeting
Long non-coding RNA
Lung cancer
MEG3
TUG1

Corresponding authors:
✉ N. Babaei
nahid.babaei@iau.ac.ir
✉ A. Jalali
a-jalali@araku.ac.ir

p-ISSN 2423-4257
e-ISSN 2588-2589

ABSTRACT

Lung cancer remains a leading cause of cancer-related mortality globally, underscoring the need for novel targeted therapies. Dysregulation of long non-coding RNAs (lncRNAs), such as the tumor suppressor *MEG3* and the context-dependent lncRNA *TUG1*, plays a critical role in non-small cell lung cancer (NSCLC) pathogenesis and chemoresistance. This study aimed to develop a targeted nanotherapeutic system to modulate these lncRNAs and selectively eliminate cancer cells. Hyaluronic acid (HA) and Gallic acid (GA)-conjugated to Glucose (Glu)-functionalized Fe_3O_4 nanoparticles (Fe_3O_4@Glu-HA-GA NPs) were synthesized and characterized by scanning electron microscopy, transmission electron microscopy, Fourier-transform infrared spectroscopy, X-ray diffraction, and thermogravimetric analyses. These nanoparticles target CD44-overexpressing cancer cells via HA functionalization. *In vitro* studies on A549 (lung adenocarcinoma) and MRC5 (normal lung fibroblast) cells revealed that Fe_3O_4@Glu-HA-GA NPs exhibited potent and selective cytotoxicity, with an IC_{50} of 70 µg/mL in A549 cells, significantly lower than in MRC5 cells (IC_{50}= 214 µg/mL). qRT-PCR analysis demonstrated a cancer cell-specific transcriptional response, where the treatment significantly upregulated *MEG3* by 1.58-fold ($p< 0.01$) and *TUG1* by 1.33-fold ($p< 0.01$) in A549 cells compared to untreated controls. This selective lncRNA dysregulation correlated with the observed anticancer activity. In conclusion, the Fe_3O_4@Glu-HA-GA nanoplatform represents a promising strategy for targeted lung cancer therapy by selectively perturbing key lncRNA networks, offering a potential avenue to overcome nonspecific toxicity and enhance therapeutic efficacy.

Please cite this paper as: Mehraban, F., Babaei, N., Jalali, A., Salehzadeh, A., & Doulah, A. (2026). Co-upregulation of *MEG3* and *TUG1* LncRNAs by hyaluronic acid-based nanoparticles confers selective toxicity in lung adenocarcinoma. *Journal of Genetic Resources,* 12(1), 41-52. doi: 10.22080/jgr.2026.31450.1459

Introduction

Lung cancer remains the most lethal malignancy, causing ~1.8 million annual deaths (Sung *et al.*, 2021). Non-small cell lung cancer (NSCLC) constitutes ~85% of cases, categorized into adenocarcinoma, squamous cell carcinoma, and large cell carcinoma (Wang *et al.*, 2020; Bade *et al.*, 2020). Despite advances in surgery, chemotherapy, radiotherapy, and targeted agents, NSCLC prognosis remains poor due to late diagnosis, tumor heterogeneity, and therapeutic resistance (Hirsch *et al.*, 2017; Zappa *et al.*, 2016), underscoring an urgent need for novel targeted strategies.

Lung cancer pathogenesis involves genetic and epigenetic alterations. Beyond tobacco smoking,

mutations in EGFR, KRAS, and ALK play critical roles in oncogenesis, particularly in non-smokers (Dan *et al.*, 2024). Long non-coding RNAs (lncRNAs) >200 nucleotides exert regulatory functions at transcriptional, post-transcriptional, and epigenetic levels (Huarte, 2015; Singh *et al.*, 2022). Their dysregulation links to tumor progression, metastasis, and drug resistance (Lin *et al.*, 2018; Sanchez-Marin *et al.*, 2022).

Among cancer-associated lncRNAs, Maternally Expressed Gene 3 (*MEG3*) and Taurine Upregulated Gene 1 (*TUG1*) have critical roles in lung cancer. *MEG3* is a tumor suppressor downregulated in NSCLC, associated with enhanced proliferation, reduced apoptosis, and cisplatin resistance. Mechanistically, *MEG3* modulates p53 signaling and regulates apoptosis- and cell cycle-related genes (Li *et al.*, 2023). *TUG1* exhibits context-dependent dual roles (oncogenic or tumor-suppressive) in various malignancies. For example, *TUG1* acts as an oncogene in glioblastoma and osteosarcoma, while it functions as a tumor suppressor in non-small cell lung cancer (NSCLC), often mediated through microRNA networks and apoptosis pathways (Gilyazova *et al.*, 2023; Liu *et al.*, 2017). Their regulatory functions underscore *MEG3* and *TUG1* as prognostic biomarkers and therapeutic targets.

However, a major challenge is targeted delivery of lncRNA-modulating agents to tumor cells while sparing healthy tissue. Conventional chemotherapy, such as cisplatin-based regimens, causes severe side effects including neuropathy, myelosuppression, and nephrotoxicity, necessitating more precise delivery systems (Chen *et al.*, 2025).

Recent studies (2024-2025) have demonstrated the efficacy of CD44-targeted nanocarriers in improving drug accumulation and therapeutic outcomes in preclinical models of non-small cell lung cancer (Zhu *et al.*, 2025; He *et al.*, 2025; Al Jayoush *et al.*, 2025). CD44-targeted nanocarriers effectively deliver therapeutics to CD44-overexpressing NSCLC cells (Zhu *et al.*, 2025). Nanotechnology offers a transformative platform: nanoparticles (NPs) enhance bioavailability, controlled release, and active targeting (Ahmad *et al.*, 2015). Superparamagnetic iron oxide nanoparticles (Fe_3O_4 NPs) are promising due to biocompatibility and magnetic properties (Fahim *et al.*, 2025; Wahajuddin *et al.*, 2012). Recent dual-targeting strategies combining CD44 and integrin receptor targeting further enhance selective uptake and efficacy in lung adenocarcinoma (He *et al.*, 2025).

Surface engineering of NPs is critical for stability and targeting. Hyaluronic acid (HA) is widely used for cancer drug delivery due to biocompatibility, biodegradability, and natural CD44 targeting. CD44 is a transmembrane glycoprotein receptor overexpressed in various tumors and inflammatory sites, acting as a master regulator of cancer stemness, metastasis, and chronic inflammation (Gama *et al.*, 2025). HA-functionalized NPs improve cellular uptake, tumor localization, and anticancer efficacy while reducing systemic toxicity, though challenges like off-target liver and spleen accumulation remain (Al Jayoush *et al.*, 2025; Andreana *et al.*, 2025). Conjugating bioactive compounds like Gallic acid (GA) synergizes therapeutic effects via oxidative stress, apoptosis, and cell cycle arrest. GA conjugation overcomes poor stability and enhances tumor-specific delivery (Holghoomi *et al.*, 2024).

Despite progress in lncRNA biology and nanodelivery, few studies have investigated actively targeted nanotherapeutics that modulate key lncRNAs as a primary mechanism. Specifically, the potential of CD44-targeted, HA and HA-conjugated to Glucose-functionalized Fe_3O_4 nanoparticles (Fe_3O_4@Glu-HA-GA NPs) to influence *MEG3* and *TUG1* expression in lung cancer remains unexplored. Comparing cancerous *vs* non-cancerous lung cells is essential for therapeutic selectivity.

Therefore, we synthesized Fe_3O_4@Glu-HA-GA NPs and evaluated cytotoxic/apoptotic effects on A549 (lung adenocarcinoma) and MRC5 (normal lung fibroblasts) cells. We investigated whether Fe_3O_4@Glu-HA-GA modulates *MEG3* and *TUG1* expression. We hypothesize selective toxicity in A549 cells. Previous studies have demonstrated the downregulation of *MEG3* and *TUG1* in NSCLC (Li *et al.,* 2016; Yang *et al.,* 2024). Consistent with these reports, our *in silico* analysis confirmed significant downregulation of both lncRNAs in NSCLC datasets. Based on these observations, we further hypothesize that therapeutic effects are mediated through restoration of these tumor-suppressive lncRNAs.

We specifically anticipate an upregulation of both *MEG3* and *TUG1* in the cancer cell line, consistent with the context-dependent tumor-suppressor role of *TUG1* highlighted by our bioinformatic data and the well-established tumor-suppressive function of *MEG3* in NSCLC. This research integrates nanotechnology with lncRNA-targeted therapy for NSCLC.

Materials and Methods

Synthesis of nanoparticles

The synthesis of the Fe_3O_4@Glu-HA-GA nanoparticles was carried out in two sequential steps. First, bare Fe_3O_4 nanoparticles (US Research Nanomaterials Inc.) were functionalized with D-glucose (Sigma-Aldrich) to introduce surface hydroxyl groups, which act as a linker for subsequent conjugation reactions. Briefly, Fe_3O_4 NPs and D-glucose at a 2:1 (w/w) ratio were dispersed in distilled water and heated at 180°C for 3 hours under continuous stirring. The resulting glucose-functionalized nanoparticles (Fe_3O_4@Glu) were collected by centrifugation, thoroughly washed with distilled water to remove unbound glucose, and dried at 70°C. In the second step, Fe_3O_4@Glu NPs (0.5 g) were mixed with HA (0.5 g, Sigma-Aldrich) and GA (0.5 g, Sigma-Aldrich) in distilled water. The suspension was sonicated for 30 minutes to ensure uniform dispersion and then incubated for 24 hours at room temperature under vigorous shaking to facilitate surface conjugation. The final Fe_3O_4@Glu nanoparticles conjugated with GA and HA (Fe_3O_4@Glu-HA-GA) were harvested by centrifugation, washed to remove unreacted components, and lyophilized for subsequent experiments.

Characterization of nanoparticles

The physicochemical properties of the synthesized Fe_3O_4@Glu-HA-GA NPs were characterized using multiple analytical techniques. Fourier-transform infrared (FT-IR) spectroscopy (Nicolet IR-100) in the range of 400–4000 cm^{-1} was employed to confirm the presence of characteristic functional groups and successful conjugation of HA and GA onto the Fe_3O_4 surface. The crystalline structure and phase composition of the nanoparticles were analyzed by X-ray diffraction (XRD) using Co-Kα radiation (λ= 1.79 Å). Surface morphology, particle size, and elemental composition were examined using field-emission scanning electron microscopy (ZEISS, Germany) and transmission electron microscopy (ZEISS, Germany). In addition, thermogravimetric analysis (TGA; Rheometric Scientific STA 1500) was performed under a nitrogen atmosphere to assess the thermal stability and estimate the organic coating content of the nanoparticles.

In silico selection of target lncRNAs

To identify lncRNAs critically involved in lung cancer pathogenesis for experimental validation, an in silico bioinformatic analysis was performed. Publicly available microarray and RNA-seq datasets comparing lung cancer samples with normal lung tissues were retrieved from the Gene Expression Omnibus (GEO) database. Differential expression analysis of lncRNAs (DElncRNAs) was conducted using the *limma* package (version 3.52.2) in R software. LncRNAs with an absolute $\log_2$ fold change ($|\log_2 FC|$)> 1 and an adjusted $p< 0.05$ were considered significantly dysregulated.

Functional enrichment analysis of the candidate DElncRNAs was subsequently performed using the LncSEA platform (version 1.0) to explore their association with cancer-related biological processes and pathways. Based on statistical significance ($p< 0.05$) in both differential expression and enrichment analyses, two lncRNAs, *MEG3* and *TUG1*, were selected as the most relevant candidates for downstream experimental evaluation.

Cell culture

The human lung adenocarcinoma cell line A549 and the normal human lung fibroblast cell line MRC5 were obtained from the Pasteur Institute of Iran. Cells were cultured in RPMI-1640 medium supplemented with 10% fetal bovine serum (FBS) and 1% penicillin/streptomycin and maintained at 37°C in a humidified incubator with 5% CO_2.

MTT cytotoxicity assay

To evaluate the cytotoxic activity of Fe_3O_4@Glu-HA-GA NPs, cells were seeded into 96-well plates at a density of ~10^4 cells per well and allowed to adhere overnight. Cells were then treated with increasing concentrations (7-500 µg/mL) of the nanoparticles. Untreated cells

served as the control group. After 24 h of incubation, the culture medium was replaced with fresh medium containing 0.5 mg/mL MTT solution, followed by incubation at 37°C for 4 h. The resulting formazan crystals were dissolved in dimethyl sulfoxide (DMSO), and absorbance was measured at 570 nm using a microplate reader. Cell inhibition was calculated using the formula: Inhibition percentage= [(OD_{570} of untreated wells - OD_{570} of treated wells)/ OD_{570} of untreated wells]× 100.

Gene expression analysis

The effects of Fe_3O_4@Glu-HA-GA NPs on the expression levels of *MEG3* and *TUG1* were evaluated by quantitative Real-time PCR. A549 cells were treated with the IC_{50} concentration of the nanoparticles for 24 hours. Total RNA was extracted using TRIzol reagent, followed by DNase I treatment to remove genomic DNA contamination. RNA concentration and purity were assessed using a NanoDrop spectrophotometer. Complementary DNA (cDNA) was synthesized from 1 µg of total RNA using a reverse transcription kit (SinaClon, Iran). qRT-PCR was performed in triplicate using SYBR Green Premix Ex Taq™ (TaKaRa, Japan). Each 10 µL reaction contained 1 µL of cDNA, 0.6 µL of each primer (5 µM), 1 µL of SYBR Green master mix, and 6.8 µL of nuclease-free water. The amplification protocol consisted of an initial denaturation at 95°C for 10 min, followed by 40 cycles of 95°C for 10 sec, 60°C for 15 sec, and 72°C for 20 sec. The *GAPDH* gene was used as the internal reference gene. Relative gene expression levels were calculated using the $2^{-\Delta\Delta Ct}$ method. Primer sequences are listed in Table 1. All primers were designed using Oligo 7 primer analysis software ver.7.60.

Table 1. Primer sequences used for qRT-PCR analysis

Target genes	Primer sequence (5′→3′)	Tm °C	Reference
MEG3	F: CTGCCCATCTACACCTCACG	64	This study
	R: CTCTCCGCCGTCTGCGCTAGGGGCT	78	This study
TUG1	F: TAGCAGTTCCCCAATCCTTG	60	This study
	R: CACAAATTCCCATCATTCC	53	This study
GAPDH	F: CCCACTCCTCCACCTTTGAC	64	Safa *et al.,* 2026
	R: CATACCAGGAAATGAGCTTGACAA	68	Safa *et al.,* 2026

Statistical analysis

All experiments were performed in at least three independent replicates, and data are presented as mean± standard deviation (SD). Statistical analyses were conducted using one-way analysis of variance (ANOVA) followed by Tukey's post hoc test for multiple comparisons in GraphPad Prism software (version 9.0). A p-value < 0.05 was considered statistically significant.

Results

Characterization of nanoparticles

The successful synthesis and conjugation of HA and GA onto Fe_3O_4 nanoparticles were confirmed through a comprehensive suite of analytical techniques. Fourier-transform infrared (FT-IR) spectroscopy verified the chemical integration of all components within the final nanoconstruct (Fig. 1). The spectrum of the final Fe_3O_4@Glu-HA-GA nanoparticles retained the defining Fe-O vibration of magnetite at 571 cm^{-1}. The concurrent presence of broad O–H/N–H stretching (3433 cm^{-1}), aliphatic C–H stretching (2925 cm^{-1}), and carbonyl C=O stretching (1628 cm^{-1}) indicated the successful incorporation of both HA and GA onto the nanoparticle surface, with peak positions showing subtle shifts consistent with molecular interactions. X-ray diffraction (XRD) analysis was employed to assess the crystalline structure (Fig. 2). The XRD profile of the final Fe_3O_4@Glu-HA-GA composite exhibited the principal diffraction peaks of magnetite, confirming the preservation of the core's crystalline phase during functionalization. A noticeable reduction in peak intensity and the appearance of a broad hump in the 15-30° 2θ range were observed, attributable to the amorphous nature of the HA coating and the integration of GA.

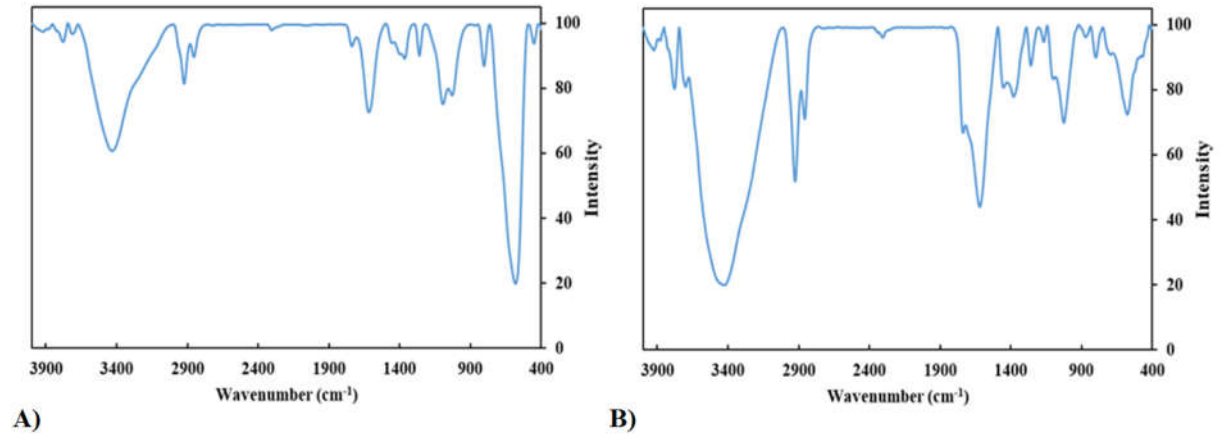

Fig. 1. Fourier-transform infrared spectra of nanoparticles: A) Fe_3O_4 nanoparticles; B) Fe_3O_4@HA-GA nanocomposite.

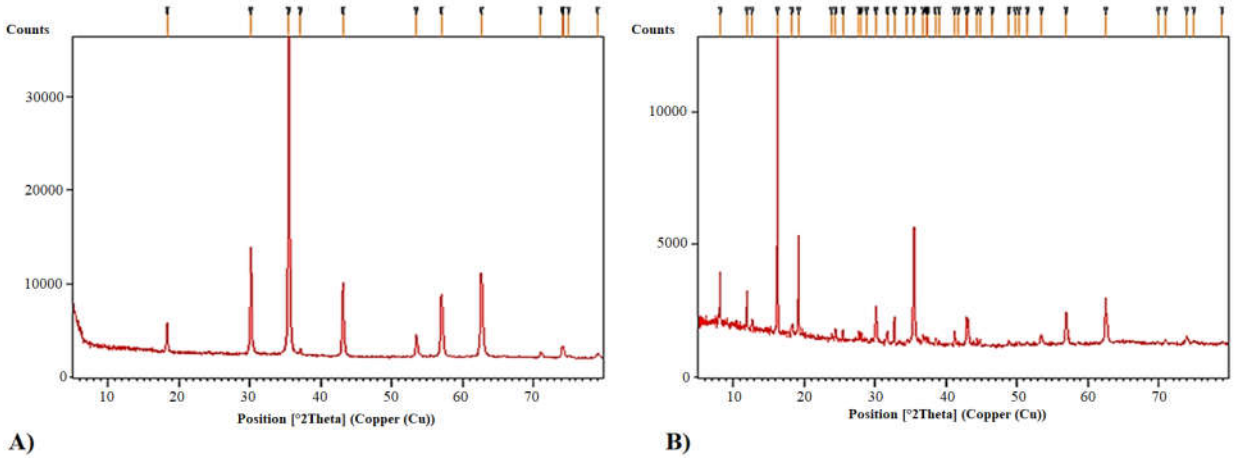

Fig. 2. X-ray diffraction patterns: A) Fe_3O_4 nanoparticles; B) Fe_3O_4@Glu-HA-GA nanoparticles.

Thermogravimetric analysis (TGA) revealed the thermal stability and organic content of the nanoparticles (Fig. 3). The Fe_3O_4@Glu-HA-GA NPs underwent a total mass loss of approximately 60.5% upon heating to 800°C. The multi-stage weight loss profile corresponded to the sequential degradation of surface-adsorbed water, the organic linker (glucose), GA, and finally the HA polymer. The remaining residue (~39.5%) was attributed to the inorganic Fe_3O_4 core, quantifying the high organic coating content.

Morphological analysis was performed by SEM and TEM. The SEM image (Fig. 4a) and TEM image (Fig. 4b) revealed that the nanoparticles were predominantly spherical with a size distribution ranging from 20 to 100 nm.

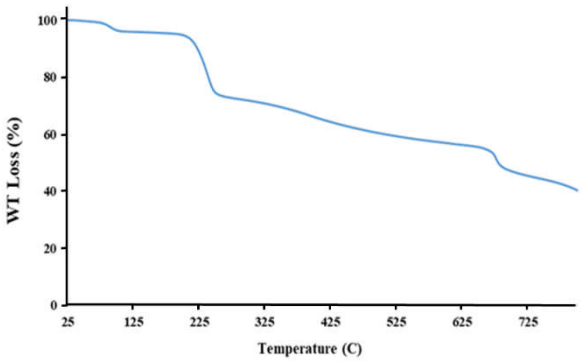

Fig. 3. Thermogravimetric analysis profile of Fe_3O_4@Glu-HA-GA nanoparticles. The vertical axis represents the percentage of weight loss (WT loss) as a function of temperature, illustrating multistep thermal decomposition and high organic content of the nanocomposite.

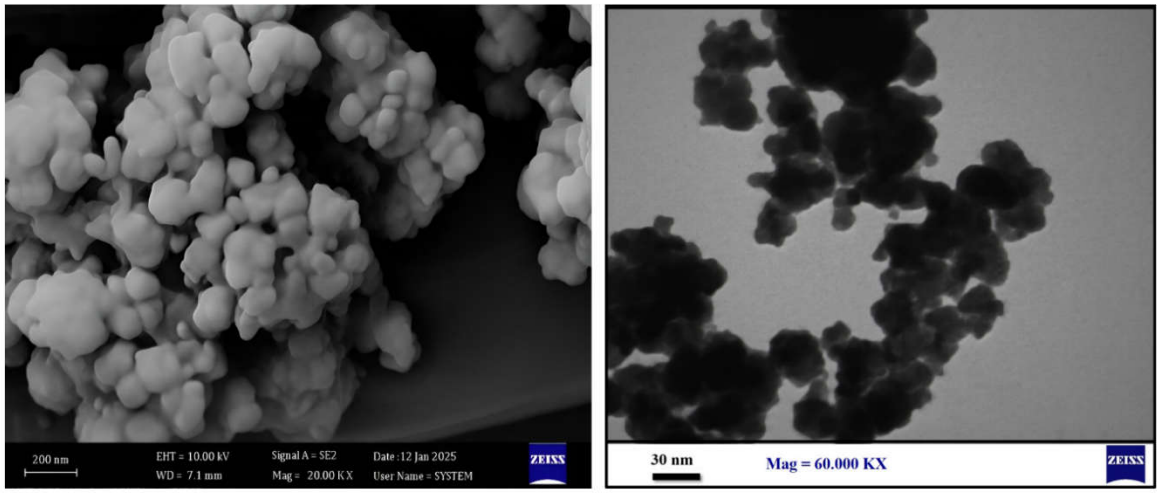

Fig. 4. Electron microscopy image of Fe_3O_4@Glu-HA-GA nanoparticles: A) Scanning electron microscopy image; B) Transmission electron microscopy image.

In Silico identification and selection of target lncRNAs

To rationally select lncRNAs for experimental investigation, a bioinformatic analysis of publicly available NSCLC transcriptomic datasets was conducted. Differential expression analysis identified 32 lncRNAs significantly dysregulated ($|\log_2FC| > 1$, $p < 0.05$) in lung cancer tissues compared to normal counterparts. The list included 14 downregulated and 18 upregulated lncRNAs. Subsequent functional enrichment analysis using the LncSEA platform prioritized lncRNAs based on their association with cancer pathways. From this analysis, *MEG3* ($\log_2FC = -3.99$) and *TUG1* ($\log_2FC = -3.35$) were selected as final candidates. Their significant downregulation in NSCLC and established roles in apoptosis and drug resistance in the literature justified their selection for evaluating the effect of our nanotherapeutic platform.

MTT assay

The antitumor efficacy and selectivity of Fe_3O_4@Glu-HA-GA NPs were evaluated using MTT assays on A549 (lung cancer) and MRC5 (normal lung fibroblast) cell lines after 24-hour exposure (Fig. 5). The NPs exhibited a dose-dependent cytotoxic effect in both cell lines. The half-maximal inhibitory concentration (IC_{50}) in A549 cancer cells was 70 µg/mL (Fig. 5a), whereas the IC_{50} in normal MRC5 cells was significantly higher at 214 µg/mL (Fig. 5b). To contextualize the therapeutic potential of the synthesized Fe_3O_4@Glu-HA-GA nanoparticles, the cytotoxicity of the conventional chemotherapeutic agent, cisplatin, was evaluated in parallel against A549 cells. Cisplatin exhibited an IC_{50} value of 69 µg/mL after 24 hours of exposure (Fig. 5c). Notably, while the absolute cytotoxic potency of our nanoformulation (IC_{50}= 70 µg/mL) is highly comparable to that of free cisplatin, the nanoparticles demonstrated an enhanced safety profile with substantially reduced toxicity toward healthy MRC5 lung fibroblasts IC_{50}= 214 µg/mL).

Gene expression analysis

The impact of Fe_3O_4@Glu-HA-GA NPs on the expression of the selected lncRNAs, *MEG3* and *TUG1*, was analyzed by qRT-PCR following a 24-hour treatment at the IC_{50} concentration (Fig. 6). In A549 cancer cells, treatment induced a significant upregulation in the expression of both lncRNAs compared to untreated controls. The tumor suppressor *MEG3* showed a 1.58-fold increase (mean± SD: 1.58± 0.09, p= 0.0088), effectively reversing the downregulation observed in the initial bioinformatic analysis of NSCLC samples. Concurrently, *TUG1* was also significantly upregulated by 1.33-fold (mean ± SD: 1.33± 0.03, p= 0.0070). This co-upregulation aligns with a desired therapeutic outcome, as both target genes are recovered from their silenced states in NSCLC tissues, prompting a joint activation of parallel anti-tumor pathways.

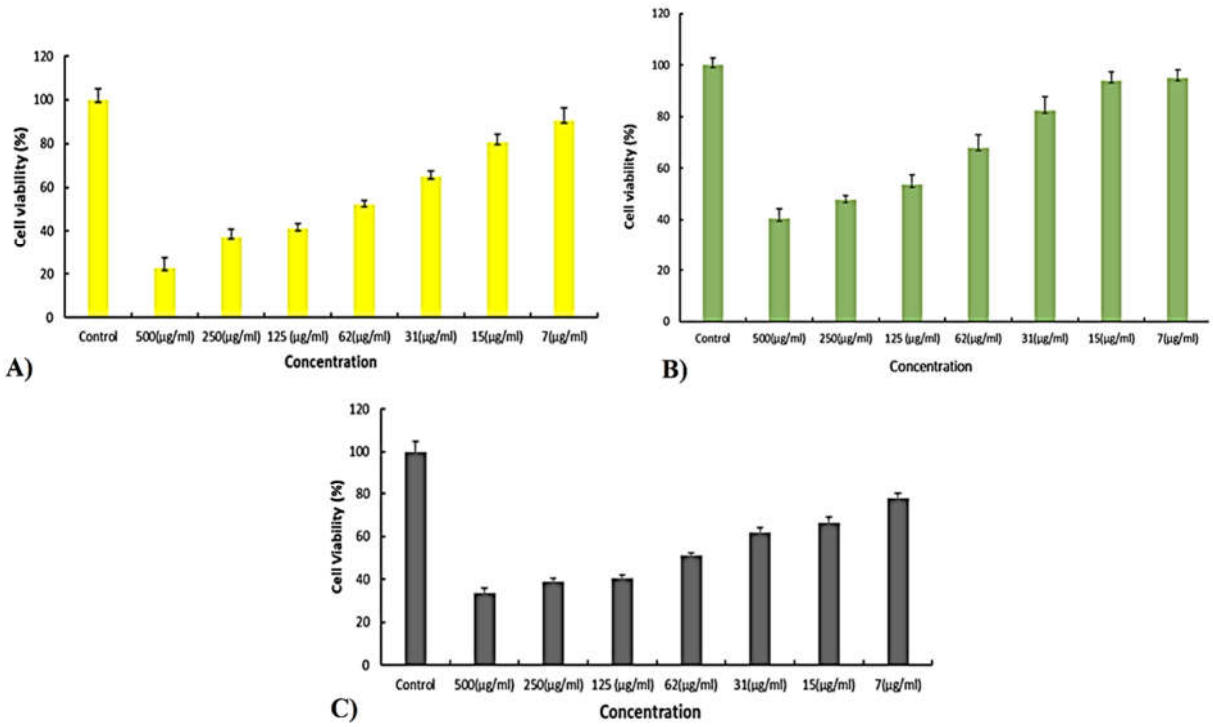

Fig. 5. Cytotoxic effects of Fe_3O_4@Glu-HA-GA nanoparticles and cisplatin on lung cancer and normal lung cells: A) Fe_3O_4@Glu-HA-GA (with IC_{50} = 70 µg/mL) on A549 cell line; B) Fe_3O_4@Glu-HA-GA (with IC_{50} = 214 µg/mL) on MRC5 cell line; C) Cisplatin (with IC_{50} = 69 µg/mL) on A549 cell line. Data are expressed as mean ± SD (n = 3).

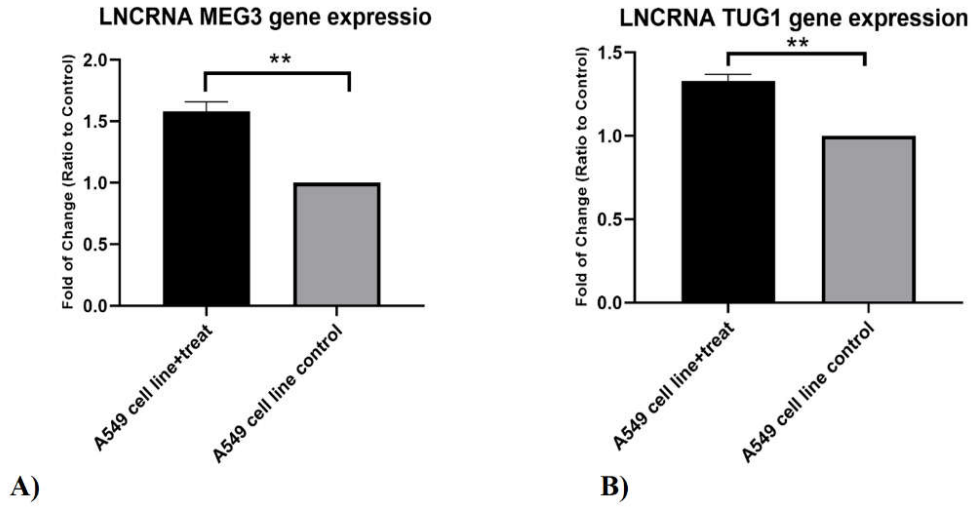

Fig. 6. Effect of Fe_3O_4@Glu-HA-GA nanoparticles on lncRNA expression in A549 lung cancer cells at 24 hours of treatment: A) Relative expression levels of *MEG3* lncRNAs; B) Relative expression levels of *TUG1* lncRNAs; Treatment was done at the IC_{50} concentration; Data are presented as mean ± SD (n= 3). **p< 0.01 and *p< 0.05 compared with untreated control cells.

Discussion

In the present study, we investigated a multifunctional nanoplatform consisting of glucose-functionalized Fe_3O_4 nanoparticles conjugated with HA and GA (Fe_3O_4@Glu-HA-GA). We focused on its selective cytotoxicity and regulatory effects on key lncRNAs in lung cancer cells. The results collectively demonstrate that this nanoconstruct not only exhibits favorable physicochemical properties but also exerts selective anticancer activity accompanied by a targeted, yet complex, dysregulation of lncRNA expression, highlighting its promise as a novel strategy for lung cancer therapy.

Comprehensive physicochemical characterization confirmed the successful integration of Fe_3O_4, glucose, HA, and GA into a single nanostructure. The preservation of the magnetite crystalline phase following surface functionalization, as evidenced by XRD analysis, is consistent with previous studies reporting that organic coating does not disrupt the core structure of Fe_3O_4-based nanocarriers (Arianna *et al.,* 2025). Furthermore, the substantial organic mass loss observed in TGA analysis supports effective surface modification, which is critical for biological interactions and therapeutic performance (Estelrich *et al.,* 2015).

One of the most notable findings of this study is the pronounced selective cytotoxicity of Fe_3O_4@Glu-HA-GA nanoparticles toward A549 lung cancer cells compared to normal MRC5 fibroblasts. This selectivity can be partly attributed to HA, a natural ligand for the CD44 receptor, which is frequently overexpressed in non-small cell lung cancer cells (Xu *et al.,* 2024; He *et al.*, 2025; Heydari *et al.*, 2025). HA-mediated CD44 targeting has been widely reported to enhance receptor-mediated endocytosis and intracellular drug accumulation in cancer cells while reducing off-target toxicity in normal tissues (Al Jayoush *et al.*, 2025; Andreana *et al.*, 2025; Mugundhan *et al.*, 2025). The higher IC_{50} value observed in MRC5 cells therefore indicates a favorable therapeutic window for the designed nanoplatform. This observation is consistent with previous studies demonstrating that nano-encapsulation of polyphenols overcomes limitations such as poor stability, rapid metabolism, and low bioavailability (You *et al.,* 2010; Li *et al.,* 2023). Importantly, the comparable cytotoxic potency of Fe_3O_4@Glu-HA-GA nanoparticles and cisplatin in A549 cells underscores the therapeutic relevance of this formulation, particularly considering its reduced toxicity toward normal lung fibroblasts.

Beyond cytotoxicity, a key strength of this study lies in elucidating a potential lncRNA-mediated mechanism underlying the observed anticancer effects. Bioinformatic analysis revealed that both *MEG3* and *TUG1* are significantly downregulated in NSCLC tissues, findings consistent with multiple transcriptomic studies (Lu *et al.,* 2013; Li *et al.,* 2023; Liu *et al.,* 2017). *MEG3* is a well-established tumor suppressor lncRNA that regulates apoptosis and cell cycle arrest through p53-dependent and independent pathways (Ghafouri-Fard *et al.,* 2019). *TUG1* has been reported to have context-dependent roles in lung cancer, potentially acting as a tumor suppressor in some studies through regulation of apoptosis and cell survival pathways (Liu *et al.,* 2017; Li *et al.,* 2021).

Experimental validation by qRT-PCR revealed that Fe_3O_4@Glu-HA-GA NPs treatment induced a significant upregulation in the expression of both selected lncRNAs in A549 cells. As anticipated based on its tumor-suppressive role, MEG3 expression increased by 1.58-fold ($p< 0.01$). The observed 1.33-fold upregulation of *TUG1* ($p< 0.01$) is consistent with our initial bioinformatic analysis, which identified significant downregulation of *TUG1* in NSCLC tissues. This finding, supported by previous experimental reports (Liu *et al.,* 2017; Gilyazova *et al.,* 2024), reinforces the putative tumor-suppressive role of *TUG1* in this specific context. Consequently, this change is more accurately interpreted as the restoration of a silenced tumor-suppressor lncRNA rather than the activation of an oncogene. The co-upregulation of both *MEG3* and *TUG1* suggests a synergistic therapeutic reactivation of parallel tumor-suppressive networks. These networks may converge on common anticancer mechanisms, including apoptosis induction and cell cycle arrest, as previously reported in NSCLC models where *TUG1* exerts tumor-suppressive functions (Zhang *et al.,* 2014; Liu *et al.,* 2017). To establish a direct causal link, future studies employing TUG1

knockdown are essential to determine whether its restoration is a mechanistic driver of the nanoplatform's cytotoxicity or a secondary biomarker of cellular response. This targeted dysregulation of key lncRNAs underscores the capacity of the Fe_3O_4@Glu-HA-GA nanoplatform to selectively reprogram the transcriptional landscape of cancer cells toward a pro-death phenotype.

It is worth noting that the qRT-PCR transcriptional analysis was exclusively conducted on the lung adenocarcinoma cell line (A549). This approach was chosen because the target lncRNAs, particularly the tumor suppressor *MEG3*, are characteristically dysregulated in cancerous states, whereas they maintain stable physiological expression in normal lung tissues. Furthermore, owing to the CD44-targeted design of the Fe_3O_4@Glu-HA-GA NPs, the therapeutic signaling cascade is selectively triggered within the cancer cells that overexpress CD44, sparing the normal MRC5 fibroblasts from significant nanoparticle internalization and subsequent genetic alterations. Such selectivity is consistent with previous reports indicating that nanoparticle-mediated gene regulation can be highly context-dependent and influenced by differential uptake and intracellular signaling between malignant and normal cells (Singh *et al.,* 2023). This selective modulation further supports the biosafety profile of the Fe_3O_4@Glu-HA-GA nanoplatform.

Despite these encouraging results, the study has several limitations that temper optimism. Notably, all experiments were conducted in vitro, limiting insights into in vivo pharmacokinetics, biodistribution, and systemic effects. Future studies should focus on evaluating the in vivo antitumor efficacy, safety profile, and biodistribution of Fe_3O_4@Glu-HA-GA NPs in orthotopic lung cancer xenograft models, as well as conducting long-term toxicity assessments prior to clinical translation. Additionally, while selective cytotoxicity and lncRNA modulation provide initial mechanistic clues, it is critical to note that the observed relationship between lncRNA changes and cytotoxicity represents a correlation rather than direct proof of causation. The exact underlying functional pathways downstream of these lncRNAs, such as the explicit involvement of apoptosis, cell cycle arrest, or reactive oxygen species (ROS) generation, remain unexplored at this stage of the study. Consequently, the current data cannot definitively establish whether the observed upregulations are the causative drivers of cancer cell death or parallel biomarkers of a broader cellular response. Future studies must incorporate mechanistic functional assays (*e.g.*, flow cytometry for apoptosis and cell cycle distribution, fluorescent ROS tracking), pathway-specific inhibitors, and gene-silencing techniques (*e.g.*, siRNA for *TUG1* or *MEG3*) to validate causality and unlock full translational potential. Collectively, these findings support a model in which HA-mediated targeting enhances nanoparticle uptake by lung cancer cells, enabling efficient intracellular delivery of GA and subsequent dysregulation of key regulatory lncRNAs, characterized by the co-upregulation of both *MEG3* and *TUG1*. This integrated mechanism highlights the potential of combining nanotechnology with lncRNA-oriented therapeutic strategies to achieve selective and effective anticancer outcomes, while also revealing the complexity of cancer cell transcriptional responses to targeted nanotherapeutics.

Conclusion

In summary, we successfully developed a CD44-targeted nanoplatform (Fe_3O_4@Glu-HA-GA) that exhibited selective cytotoxicity against A549 lung cancer cells over normal MRC5 fibroblasts, largely due to HA-mediated active targeting. Crucially, and in line with our bioinformatic findings, the treatment selectively restored the expression of two key tumor-suppressive lncRNAs, *MEG3* and *TUG1*, which are commonly silenced in NSCLC. This co-restoration suggests a unified therapeutic mechanism wherein the Fe_3O_4@Glu-HA-GA nanoplatform concurrently reactivates multiple silenced tumor-suppressive pathways, culminating in selective cytotoxicity against lung adenocarcinoma cells. This positions the nanoplatform as a targeted epigenetic/transcriptional modulator that leverages receptor-mediated uptake to reverse a disease-specific gene silencing pattern. These findings highlight the potential of targeted nano therapy to precisely reprogram key lncRNA networks in cancer cells, providing a promising

strategy for NSCLC treatment that warrants further *in vivo* investigation.

Conflict of interests

The authors declare no conflict of interest.

References

Ahmad, J., Akhter, S., Rizwanullah, M., Amin, S., Rahman, M., Ahmad, M. Z., ... & Ahmad, F. J. (2015). Nanotechnology-based inhalation treatments for lung cancer: state of the art. *Nanotechnology, Science and Applications*, 8, 55-66. https://doi.org/10.2147/NSA.S49052

Al Jayoush, AR., Haider, M., Khan, SA., & Hussain, Z. (2025). Hyaluronic acid-functionalized nanomedicines for CD44-receptors-mediated targeted cancer therapy: A review of selective targetability and biodistribution to tumor microenvironment. *International Journal of Biological Macromolecules,* 308(2), 142486. https://doi.org/10.1016/j.ijbiomac.2025.142486

Andreana, I., Zoratto, N., Di Meo, C., Matricardi, P., Stella, B., & Arpicco, S. (2025). An overview of hyaluronic-acid nanoparticles for cancer cell targeted drug delivery. *Expert Opinion on Drug Delivery*, 22(9), 1257-1274. https://doi.org/10.1080/17425247.2025.2515266

Arianna, F., Safriani, L., Kusumadewi, A. N., Gultom, N. S., Risdiana, & Saragi, T. (2025). *In situ* surface modification by oleic acid of magnetite nanoparticles: surface interaction, structure, and its magnetic properties. *Journal of Materials Science: Materials in Engineering*, 20(1), 87. https://doi.org/10.1186/s40712-025-00303-x

Bade, B. C., & Cruz, C. S. D. (2020). Lung cancer 2020: epidemiology, etiology, and prevention. *Clinics in Chest Medicine*, 41(1), 1-24. https://doi.org/10.1016/j.ccm.2019.10.001

Chen, K. W., Huang, H. L., Wang, C. C., Hsiao, C. H., Lee, Y. C., Lu, Z. B., ... & Lin, Y. H. (2025). Innovative design of hyaluronic acid conjugated polymeric drug for targeted therapy of non-small cell lung cancer. *International Journal of Biological Macromolecules*, 318, 144874. 144874. https://doi.org/10.1016/j.ijbiomac.2025.144874

Dan, A., Burtavel, L. M., Coman, M. C., Focsa, I. O., Duta-Ion, S., Juganaru, I. R., ... & Radoi, V. E. (2024). Genetic blueprints in lung cancer: Foundations for targeted therapies. *Cancers*, 16(23), 4048. https://doi.org/10.3390/cancers16234048

Estelrich, J., Escribano, E., Queralt, J., & Busquets, M. A. (2015). Iron oxide nanoparticles for magnetically-guided and magnetically-responsive drug delivery. *International Journal of Molecular Sciences*, 16(4), 8070-8101. https://doi.org/10.3390/ijms16048070

Fahim, Y. A., Hasani, I. W., & Mahmoud Ragab, W. (2025). Promising biomedical applications using superparamagnetic nanoparticles. *European Journal of Medical Research*, 30(1), 441. https://doi.org/10.1186/s40001-025-02696-z

Gama, J. M., & Oliveira, R. C. (2025). CD44 and its role in solid cancers-A review: From tumor progression to prognosis and targeted therapy. *Frontiers in Bioscience-Landmark*, 30(3), 24821. https://doi.org/10.31083/FBL24821

Ghafouri-Fard, S., & Taheri, M. (2019). Maternally expressed gene 3 (MEG3): A tumor suppressor long non coding RNA. *Biomedicine and Pharmacotherapy*, 118, 109129. https://doi.org/10.1016/j.biopha.2019.109129

Gilyazova, I., Gimalova, G., Nizamova, A., Galimova, E., Ishbulatova, E., Pavlov, V., & Khusnutdinova, E. (2023). Non-coding RNAs as key regulators in lung cancer. *International Journal of Molecular Sciences*, 25(1), 560. https://doi.org/10.3390/ijms25010560.

He, J., Li, T., Pan, X., Deng, Z., Huang, J., Mo, X., ... & Yang, J. (2025). CD44 and αV-integrins dual-targeting bimetallic nanozymes for lung adenocarcinoma therapy via NIR-enhancedferroptosis/apoptosis. *Biomaterials*, 323, 123407. https://doi.org/10.1016/j.biomaterials.2025.123407

Heydari, M., Colagar, A. H. & Sabour, D. (2025). Anti-proliferative and anti-migratory effects of Urtica dioica agglutinin loaded chitosan nanoparticles with hyaluronic acid coating on the CD44-overexpressing prostate cancer cells. International Journal of Environmental Health Research. 35(10):2929-2943 https://doi.org/10.1080/09603123.2025.2465877

Hirsch, F. R., Scagliotti, G. V., Mulshine, J. L., Kwon, R., Curran, W. J., Wu, Y. L., & Paz-Ares, L. (2017). Lung cancer: Current therapies and new targeted treatments. *The*

Lancet, 389(10066), 299-311. https://doi.org/10.1016/S01406736(16)30958-8

Holghoomi, R., Kiani, M. H., Rahdar, A., Hashemi, S. M., Ferreira, L. F. R., & Fathi-karkan, S. (2024). Nanoparticle-delivered gallic acid: A new frontier in cancer therapy. *Journal of Drug Delivery Science and Technology*, 101, 106129. https://doi.org/10.1016/j.jddst.2024.106129

Huarte, M. (2015). The emerging role of lncRNAs in cancer. *Nature Medicine*, 21(11), 1253-1261.1261. https://doi.org/10.1038/nm.3981

Li, K., Gong, Q., Xiang, X. D., Guo, G., Liu, J., Zhao, L., ... & Zhuang, L. (2023). HNRNPA2B1-mediated m6A modification of lncRNA MEG3 facilitates tumorigenesis and metastasis of non-small cell lung cancer by regulating miR-21-5p/PTEN axis. *Journal of Translational Medicine*, 21(1), 382. https://doi.org/10.1186/s12967-023-04190-8

Li, K., Niu, H., Wang, Y., Li, R., Zhao, Y., Liu, C., ... & Zhuang, L. (2021). LncRNA *TUG1* contributes to the tumorigenesis of lung adenocarcinoma by regulating miR-138-5p-HIF1A axis. *International Journal of Immunopathology and Pharmacology*, 35, 20587384211048265. https://doi.org/10.1177/20587384211048265

Li, N., Wang, C., Feng, B., Bi, Y., Kong, F., Wang, Z., & Tan, S. (2023). Application of nanoencapsulation technology to improve the stability and bioactivity of tea polyphenols. *Food Bioscience*, 55, 103076. https://doi.org/10.1016/j.fbio.2023.103076

Li, Z., Shen, J., Chan, M. T., & Wu, W. K. K. (2016). TUG 1: A pivotal oncogenic long non-coding RNA of human cancers. *Cell Proliferation*, 49(4), 471-475. https://doi.org/10.1111/cpr.12269

Lin, C., & Yang, L. (2018). Long noncoding RNA in cancer: wiring signaling circuitry. *Trends in Cell Biology*, 28(4), 287-301. https://doi.org/10.1016/j.tcb.2017.11.008

Liu, H., Zhou, G., Fu, X., Cui, H., Pu, G., Xiao, Y., ... & Yang, X. (2017). Long noncoding RNA TUG1 is a diagnostic factor in lung adenocarcinoma and suppresses apoptosis via epigenetic silencing of BAX. *Oncotarget,* 8(60), 101899. https://doi.org/10.18632/oncotarget.22058

Lu, K. H., Li, W., Liu, X. H., Sun, M., Zhang, M. L., Wu, W. Q., ... & Hou, Y. Y. (2013). Long non-coding RNA *MEG3* inhibits NSCLC cells proliferation and induces apoptosis by affecting p53 expression. *BMC cancer*, 13(1), 461. https://doi.org/10.1186/1471-2407-13-461

Mugundhan, S. L., & Mohan, M. (2025). Hyaluronic acid-coated capecitabine nanostructures for CD44 receptor-mediated targeting in breast cancer therapy. *RSC Advances*, 15(16), 12653-12670. https://doi.org/10.1039/d5ra01275a

Safa, A., Shafiei, M., Sangari, A. N., Roudbordeh, A. N., Ghaderibarmi, F., Kohsarian, M., ... & Salehzadeh, A. (2025). Targeted anticancer effects of Juglone-ZnO nanoparticles via cell cycle arrest and caspase-mediated apoptosis in colon cancer cells. *Scientific Reports*. https://doi.org/10.1038/s41598-025-31183-y

Sanchez-Marin, D., Trujano-Camacho, S., Perez-Plasencia, C., De Leon, D. C., & Campos-Parra, A. D. (2022). LncRNAs driving feedback loops to boost drug resistance: sinuous pathways in cancer. *Cancer Letters*, 543, 215763. https://doi.org/10.1016/j.canlet.2022.215763

Singh, D., Assaraf, Y. G., & Gacche, R. N. (2022). Long non-coding RNA mediated drug resistance in breast cancer. *Drug Resistance Updates*, 63, 100851. https://doi.org/10.1016/j.drup.2022.100851

Singh, G., Dasanayake, G. S., Chism, C. M., Vashisth, P., Kaur, A., Misra, S. K., ... & Tanner, E. E. (2023). Good's buffer based highly biocompatible ionic liquid modified PLGA nanoparticles for the selective uptake in cancer cells. *Materials Chemistry Frontiers*, 7(24), 6213-6228. https://doi.org/10.1039/d3qm00787a

Sung, H., Ferlay, J., Siegel, R. L., Laversanne, M., Soerjomataram, I., Jemal, A., & Bray, F. (2021). Global cancer statistics 2020: GLOBOCAN estimates of incidence and mortality worldwide for 36 cancers in 185 countries. *Cancer Journal for Clinicians*, 71(3), 209-249. https://doi.org/10.3322/caac.21660

Wahajuddin, N., & Arora, S. (2012). Superparamagnetic iron oxide nanoparticles: magnetic nanoplatforms as drug carriers.

International Journal of Nanomedicine, 7, 3445-3471. https://doi.org/10.2147/IJN.S30320

Wang, B. Y., Huang, J. Y., Chen, H. C., Lin, C. H., Lin, S. H., Hung, W. H., & Cheng, Y. F. (2020). The comparison between adenocarcinoma and squamous cell carcinoma in lung cancer patients. *Journal of Cancer Research and Clinical Oncology*, 146(1), 43-52. https://doi.org/10.1007/s00432-019-03079-8

Xu, Y., Benedikt, J., & Ye, L. (2024). Hyaluronic acid interacting molecules mediated crosstalk between cancer cells and microenvironment from primary tumour to distant metastasis. *Cancers*, 16(10), 1907. https://doi.org/10.3390/cancers16101907

Yang, Y., Tian, Z., He, L., Meng, H., Xie, X., Yang, Z., ... & Huang, C. (2024). RhoGDIβ inhibition via miR-200c/AUF1/SOX2/miR-137 axis contributed to lncRNA MEG3 downregulation-mediated malignant transformation of human bronchial epithelial cells. *Molecular Carcinogenesis*, 63(5), 977-990. https://doi.org/10.1002/mc.23702

You, B. R., Kim, S. Z., Kim, S. H., & Park, W. H. (2011). Gallic acid-induced lung cancer cell death is accompanied by ROS increase and glutathione depletion. *Molecular and Cellular Biochemistry*, 357(1), 295-303. https://doi.org/10. 1007/s11010-011-0900-8

Zappa, C., & Mousa, S. A. (2016). Non-small cell lung cancer: current treatment and future advances. *Translational Lung Cancer Research*, 5(3), 288. https://doi.org/10.21037/tlcr.2016.06.07

Zhu, N., Guo, R., Jiang, Y., & Xu, M. (2025). CD44 targeted functionalized nanocarriers for non-small cell lung cancer. *Frontiers in Oncology*, 15, 1692667. https://doi.org/10.3389/fonc.2025.1692667